Available online at www.sciencedirect.com
ScienceDirect
Trans. Nonferrous Met. Soc. China 23(2013) 1543−1548
Transactions of Nonferrous Metals Society of China
www.tnmsc.cn

Evolution behavior of TiB_2 particles during laser welding on aluminum metal matrix composites reinforced with particles

Chao MENG, Hai-chao CUI, Feng-gui LU, Xin-hua TANG

Shanghai Key Laboratory of Materials Laser Processing and Modification,
School of Materials Science and Engineering, Shanghai Jiao Tong University, Shanghai 200240, China

Received 2 May 2012; accepted 18 June 2012

Abstract: The evolution behavior of TiB_2 particles was studied during laser welding on aluminum metal matrix composites (MMCs) reinforced with TiB_2 particles by a high power laser. X-ray diffractometry (XRD), scanning electron microscopy (SEM) and energy spectrum analysis (EDS) were used to analyze the phase, thermodynamics and morphology characteristics of the particles in the weld seam, and the interface reactions between TiB_2 particles and aluminum matrix were also discussed. The results show that partial TiB_2 particles melt and merge into larger ones in the middle of the weld seam and that fracture can be found in larger particles when the scale of TiB_2 cluster is larger than the spot size of laser. Al_3Ti and AlB_{12} are produced by the interface reaction between TiB_2 particles and Al matrix. The interface reaction of broken TiB_2 particles in the middle of the weld seam is stronger than that at the edge of the weld seam.

Key words: metal matrix composites; TiB_2 particles; laser welding; interface reaction

1 Introduction

With the development of industry and technology, the special materials are required in the fields such as aerospace, aviation and automobile. Aluminum metal matrix composites (MMCs) reinforced with particles for their low density, high strength and high modulus, good wearing resistance become one of the most promising materials. However, there are a lot of difficulties in welding Al MMCs, such as brittle phase Al_4C_3 or brittle spinel laser $MgAl_2O_4$ produced in welding Al MMCs reinforced with particles like SiC or Al_2O_3, which can reduce the mechanical properties of the welding joint [1−3]. Many methods were used to prevent the formation of a brittle phase or layer. Elements Si and Ti could be added into SiC-reinforced Al composites to inhibit the interface reaction between SiC and Al to ensure the weld joint quality [4−6]. TiB_2-reinforced particulate Al MMCs have higher strength, better wearing resistance and compatibility between the reinforced phase and the matrix compared with Al matrix composites reinforced with other particulates. Welding plays an important role in enlarging the applications, but the weldability of TiB_2-reinforced Al MMCs was rarely reported. VIJAY and MURUGAN [7] studied the mechanical properties of friction stir welded Al−10%TiB_2 (mass fraction) metal matrix composites. It was found that TiB_2 particulates homogeneously distributed both in the weld zone and Al matrix. NAHED et al [8] found that Al_3Ti and AlB_{12} were produced in the process of in-situ preparation of TiB_2-reinforced Al matrix composites through the reaction between molten Al and K_2TiF_6 and KBF_4, which caused the decrease of the reinforcement effect of TiB_2 particles. In addition, TiB_2 will be easily oxidized into TiO_2 and B_2O_3 in the air at elevated temperature [9]. Compared with traditional welding methods, laser welding becomes an increasingly significant joint technique for its higher power density, deeper penetration and higher efficiency. Laser welding on particles reinforced Al composites is becoming a new research focus. CUI et al [10] studied TiB_2 particle distribution and the reaction possibility between the reinforced phase and the matrix in the weld seam by laser full-penetration welding on in-situ TiB_2-reinforced Al composites. It was found that there is no obvious

Foundation item: Project (11ZR1417500) supported by the Natural Science Foundation of Shanghai, China; Project(51035004) supported by the National Natural Science Foundation of China
Corresponding author: Feng-gui LU; Tel: +86-21-54748940-8025; E-mail: lfg119@sjtu.edu.cn
DOI: 10.1016/S1003-6326(13)62628-X

evidence for the reaction between TiB_2 particles and Al matrix and also TiB_2 particles distribute more uniformly in the seam compared with the base metal.

It is known that the reinforced particles as ceramic phase possess higher electric resistance which is proportional to the absorption rate to laser. So, when the cluster size of reinforcement is larger than the laser spot size, which is possible for the composites reinforced by high volume fraction particles, the temperature of particles increases promptly due to the high absorption and the low thermal conductivity. But there are few researches reported about TiB_2 cluster's evolution behavior in the laser welding process of Al MMCs. In order to study the behavior of TiB_2 particles with larger cluster size than the laser spot size, an Al matrix composite with 1−5 μm TiB_2 particles and ZL101 alloy was particularly designed in this work to explore the evolution of TiB_2 particles. And also the behavior of TiB_2 particles with a high volume fraction in the laser welding process was studied, and the interface reaction between TiB_2 particles and Al matrix was discussed to obtain a high quality weld joint of Al MMCs reinforced with higher volume fraction of TiB_2 particles.

2 Experimental

15 kW CO_2 laser welding system with a spot diameter of 0.8 mm was used to weld the TiB_2−ZL101 composite. Pure helium as shielding gas with a flow rate of 28 L/min was ejected by a forward nozzle inclining to the beam axis for 45°. Self-manufactured TiB_2−ZL101 composites were employed. Small holes were made inside the specimens with the dimensions of *d*2 mm× 2 mm in the middle of the up face to remove the internal gas in materials in vacuum. The surface of specimens was machined to remove the oxide film surface and cleaned with acetone. After desiccating for 2 h, the specimens were compressed tightly with smooth ZL101 plates to make sure of no gap between up and down plates in the welding process. The welding specimen filled with TiB_2 particles in the middle of plates is shown in Fig. 1. The chemical composition of ZL101 matrix is shown in Table 1.

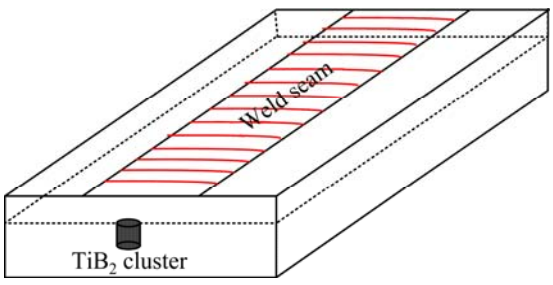

Fig. 1 Model of welding specimen

Table 1 Composition of ZL101 matrix (mass fraction, %)

Si	Mg	Zr	Fe	Al
6.67	0.45	0.42	0.14	Bal.

The microstructure and EDS analysis of TiB_2 particles are shown in Fig. 2. It is found from Fig. 2 that the size range of TiB_2 particles is from 1 to 5 μm, and no other impurity elements are detected.

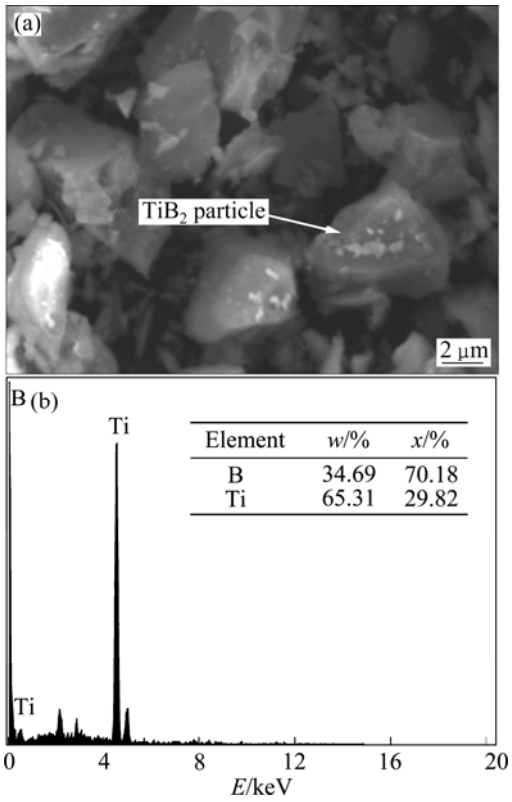

Fig. 2 Microstructure (a) and EDS analysis (b) of TiB_2 particles

3 Results and discussion

3.1 Phase and thermodynamics analysis of weld seam

The XRD pattern (Fig. 3) shows the possibility of the presence of Al_3Ti, B_2O_3, AlB_{12} and TiO_2 in the weld seam. It illustrates that TiB_2 particles are evolved into TiO_2 and B_2O_3 through the reaction with oxygen molecules in the laser welding process, as shown in Reaction (1). With increasing the temperature, Ti and B ions are released from the broken Ti—B covalent bonds and diffuse into liquid Al, which causes the formation of AlB_{12} and Al_3Ti in the reaction with Al matrix, as shown in Reactions (2) and (3).

$$TiB_2(s)+(5/2)O_2(g)\rightarrow TiO_2(s)+B_2O_3(g) \quad (1)$$

$$Al+12[B]\rightarrow AlB_{12} \quad (2)$$

$$3Al+[Ti]\rightarrow Al_3Ti \quad (3)$$

In order to evaluate the stability of the precipitated phases, it is crucial to have a reliable calculation for the

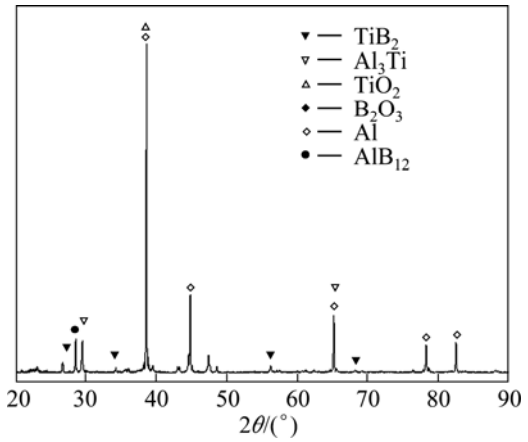

Fig. 3 XRD pattern of weld seam

Gibbs free energy change ΔG in Reactions (1) to (3). In these reactions, ΔG is not only dependent on temperature but also on the concentration of reactants and products. Therefore, the Gibbs free energy change of Reactions (1) to (3) can be expressed as:

$$\Delta G_{TiO_2}+\Delta G_{B_2O_3}=\Delta G^{\Theta}_{TiO_2}+\Delta G^{\Theta}_{B_2O_3}-RT\ln\alpha_{Ti}-2RT\ln\alpha_{B}-5RT\ln\alpha_{O} \quad (4)$$

$$\Delta G_{AlB_{12}}=\Delta G^{\Theta}_{AlB_{12}}-RT\ln\alpha_{Al}-12RT\ln\alpha_{B} \quad (5)$$

$$\Delta G_{Al_3Ti}=\Delta G^{\Theta}_{Al_3Ti}-3RT\ln\alpha_{Al}-RT\ln\alpha_{Ti} \quad (6)$$

where ΔG^{Θ} is the standard Gibbs free energy change, for the standard Gibbs free energy change of different substances, the ΔG^{Θ} values are listed in Table 2 [11,12]; and α_i represents the activity of component i in the melting composite. The activities of products TiO_2, B_2O_3, AlB_{12} and Al_3Ti in molten Al can be approximate to unity. So, the Gibbs free energy change of Reactions (1) to (3) approximately equals the standard Gibbs free energy change of different substances.

Table 2 ΔG^{Θ} values of TiO_2, Al_3Ti, B_2O_3 and AlB_{12} [11,12]

No.	Reaction	ΔG^{Θ} expression/(J·mol^{-1})
1	$TiB_2(s)+5/2O_2(g)\rightarrow TiO_2(s)+B_2O_3(g)$	$-1470544.4+124.2T$
2	$Al+12[B]\rightarrow AlB_{12}$	$-220000+7.5T$
3	$Al+[Ti]\rightarrow Al_3Ti$	$-144242+21T$

The curves between the Gibbs free energy change of reactions and temperature are shown in Fig. 4. It can be seen that the Gibbs free energies change of all reactions are negative below 3000 K, so these reactions are possible to occur with the negative Gibbs free energy in the laser welding process. Although the above results are obtained under the circumstance of equilibrium thermodynamics, they can also theoretically illustrate the possibility and the trend of oxidation reaction between TiB_2 particles and O_2 existing in air or dissolving in the molten pool and interface reaction between TiB_2 and molten Al under the circumstance of nonequilibrium thermodynamics in this work. The products are TiO_2 and B_2O_3 in oxidation reaction and AlB_{12} and Al_3Ti in interface reaction, respectively.

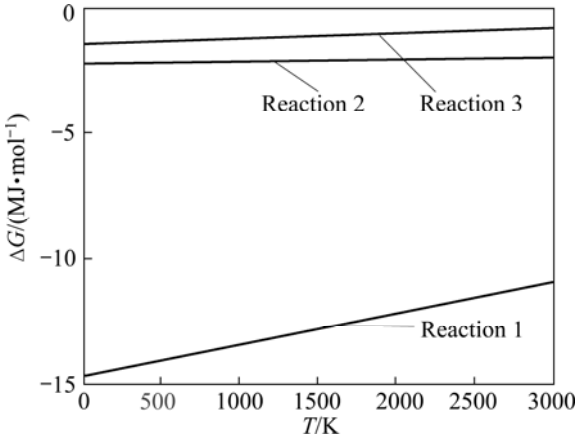

Fig. 4 Curves of ΔG versus temperature

According to the reaction kinetics, chemical reactions rely on the diffusion of atoms. The above reactions illustrate that TiB_2 particles melt during the welding process, which promotes the diffusion of Ti, B, Al and O atoms. As the maximum temperature of the molten pool except for the keyhole during the welding is under the boiling point of Al (2740 K), the negative Gibbs free energy change promotes the molten TiB_2 to react with Al and O atoms.

3.2 Microstructure and interface reaction of weld seam

Figure 5 shows the microstructures of the weld seam observed by a JSM−6460 SEM. The TiB_2 particles blocked together inside the weld seam have a distinct boundary with Al matrix due to more concentrated energy in the center of the welding section, as shown in Fig. 5(a). There are no distinct boundaries between large scale TiB_2 blocky structures. From Fig. 5(b), it can be seen that the fracture occurs on TiB_2 particles with larger radius to some extent. In this situation, some Al can be found among TiB_2 particles. TiB_2 would be irradiated by laser when the volume fraction of TiB_2 clusters in the weld seam is large enough, which causes the temperature of TiB_2 clusters to increase sharply and transfer energy to surrounding Al matrix, leading to the melting of TiB_2 clusters and the breakage of covalent bonds between Ti and B.

3.2.1 Melting of TiB_2 particles

EDS analysis was performed to analyze the molten TiB_2 in the weld seam, as shown in Fig. 6. It can be seen

that Ti and B elements are accounted for the vast majority of mass. The laser beam irradiates TiB_2 powder band completely because its width (2 mm) is far larger than the diameter of the laser spot (0.8 mm). So it is reasonable that TiB_2 particles in melting merge together in high density energy. As the thermal conductivity of the TiB_2 particles (25 W/(m·K)) is far less than that of Al (151 W/(m·K)) and the accumulation of TiB_2 particles is porous, which makes that energy cannot be transferred timely from TiB_2 particles to Al matrix in the laser welding process of TiB_2/ZL101 MMCs. The surrounding Al matrix around molten TiB_2 particles vaporizes or reacts with TiB_2 due to its drastic flow in the molten pool. Therefore, TiB_2 particles are pushed away from the keyhole region by the reaction force of Al evaporation before Al liquid enters the keyhole region and re-solidifies to large scale TiB_2 blocky structures. The results show that TiB_2 particles will melt and re-solidify when the size of TiB_2 particles cluster is larger than that of laser beam in the laser welding process.

Although TiB_2 particles are not directly irradiated by the laser in this work, the keyhole is complete within the area of TiB_2 particles in the welding process, which leads to sharp temperature elevation and weak convection, further to the melting of TiB_2 particles and a series of evolution of TiB_2.

3.2.2 Fracture of TiB_2 particles

As the laser energy absorption rate of TiB_2 particles is far greater than that of Al matrix, the evolution of TiB_2 will be influenced dramatically if TiB_2 particles are exposed directly to the laser energy in the welding process. According to Ref. [13], the bond energies of Ti—Ti, Ti—B and B—B are 0.162, 0.13 and 0.967 eV, respectively. So, the covalent bond of Ti—B will be the most likely to crack with the decrease of stability of TiB_2. Some broken TiB_2 particles are found in the weld seam in Fig. 5(b). The microstructure and EDS analysis of the broken TiB_2 particles are shown in Fig. 7. A small quantity of Al element is found on the surface of TiB_2 particles, which indicates that new phase is probably generated from the interface reaction between TiB_2 particles and Al matrix in the laser welding process.

TiB_2 particles located in the keyhole wall were heated to high temperature rapidly because of direct irradiation of laser, which moved into liquid Al at the evaporation force and cooled rapidly with laser welding process going on. Different local temperatures of TiB_2 particles due to rapid heating and cooling induced thermal stress within unevenly expanded TiB_2 particles, which made these particles break when the stress reached a critical value. The thermal stress (p) [14] in materials can be expressed as

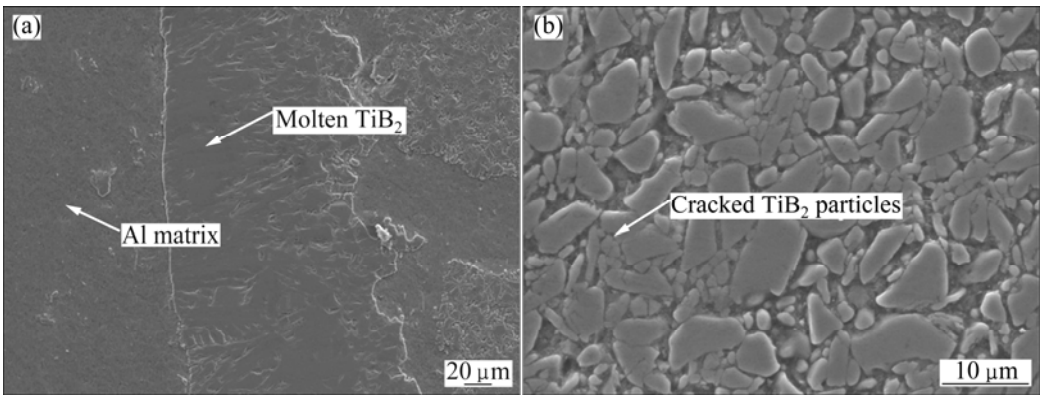

Fig. 5 Microstructures of weld seam: (a) Lower magnification; (b) Higher magnification

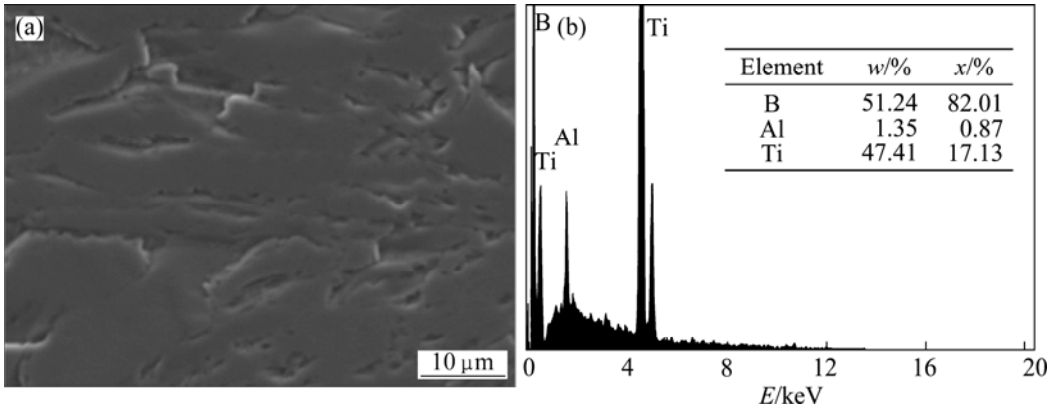

Fig. 6 Microstructure (a) and EDS analysis (b) of molten TiB_2 in weld seam

$$p = 2E\Delta\alpha\Delta T / 3(1-\nu) \quad (7)$$

where $\Delta\alpha$ is the difference of thermal expansion coefficients due to different temperatures, ΔT is the change of the temperature, ν is the Poisson ratio, and E is the elastic modulus of TiB_2 particles.

So, the thermal stress becomes increasingly greater with larger temperature difference within the particles, which leads to the breakage of Ti—B covalent bonds and the fragmentation of TiB_2 particles finally.

3.2.3 Interface reaction in weld seam

As shown in Fig. 8, the microstructure of some TiB_2 particles is distinct from the others, indicating that the TiB_2 particles semi-fuse with Al matrix. According to the EDS analysis and also combined with the XRD analysis above, Al_3Ti is preliminarily judged as the produced phase in the welding process, which illustrates that the molten TiB_2 reacts with Al matrix. Based on the Gibbs free energy change curve in Fig. 4, the reaction is feasible. In addition, the product of the reaction might consist of the mixture of AlB_{12} and Al_3Ti, as AlB_{12} is confirmed by XRD analysis and three elements of Al, Ti and B are also found in EDS spectra of some particles.

The microstructure at the edge of the weld seam is shown in Fig. 9. Although TiB_2 particles located at the edge of the weld seam experience the interface reaction

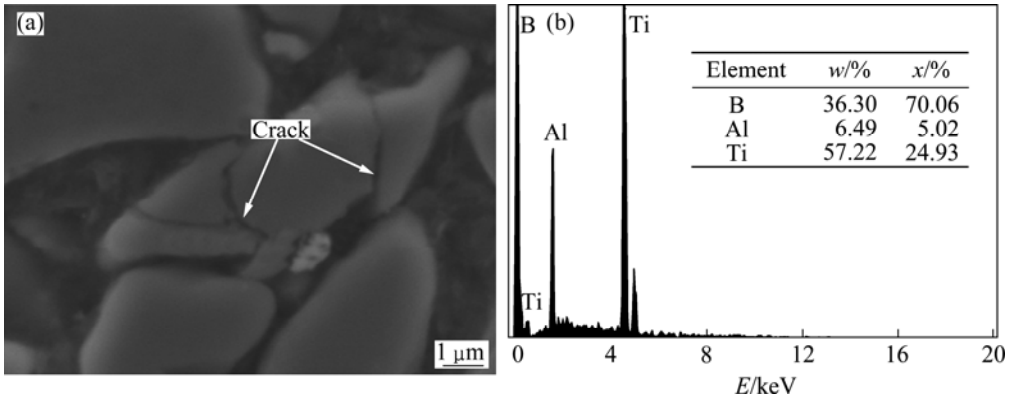

Fig. 7 Microstructure (a) and EDS analysis (b) of cracked TiB_2 particles

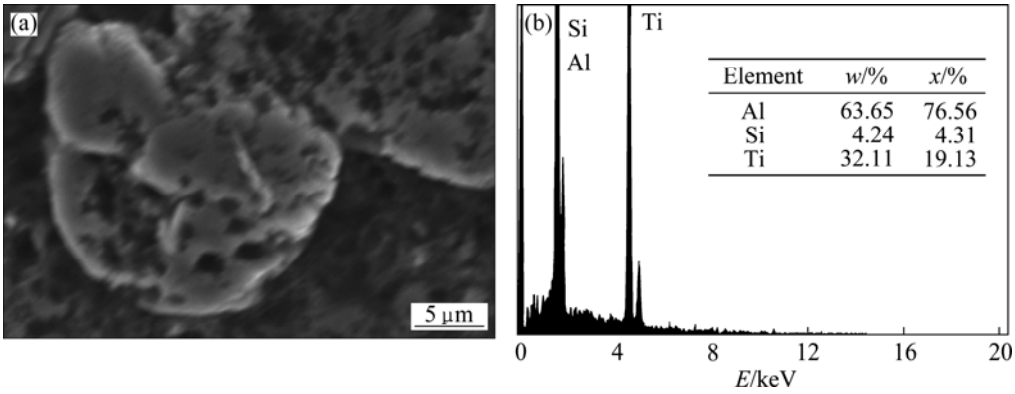

Fig. 8 Microstructure (a) and EDS analysis (b) of product of TiB_2 particles and Al matrix

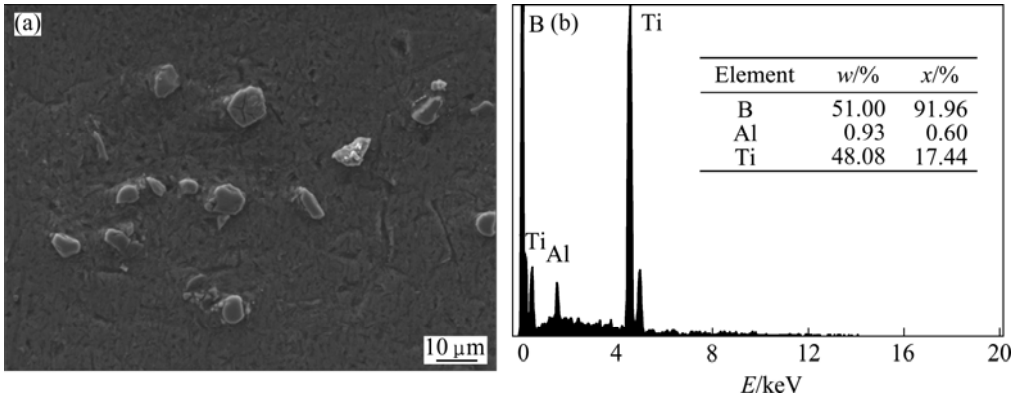

Fig. 9 Microstructure (a) and EDS analysis (b) of TiB_2 particles at edge of weld seam

based on the EDS spectrum, the mass fraction of Al element is far less than that of TiB_2 particles in the middle of the weld seam. For the high energy density of the laser, the interface reaction between TiB_2 particles and Al matrix is sufficient. As the laser energy subjects to a Gaussian distribution, the interface reaction of the broken TiB_2 particles in the middle of the weld seam is stronger than that at the edge of the weld seam.

4 Conclusions

1) TiB_2 particles merge into large blocks when rare Al liquid moves into the molten TiB_2 clusters. Small Al liquid can move into the molten TiB_2 clusters. TiB_2 particles will not merge into large ones but fracture in larger ones.

2) When TiB_2 particles melt and encounter the Al liquid, the interface reaction occurs and AlB_{12} and Al_3Ti are produced. For the high energy density of the laser beam that subjects to a Gaussian distribution, the interface reaction of the broken TiB_2 particles in the middle of the weld seam is stronger than that at the edge of weld seam.

3) For the Al matrix composites with high volume reinforcement, the laser welding technology probably produces the poor welding properties.

References

[1] LLOYD D J. Particle reinforced aluminum and magnesium matrix composites [J]. International Materials Reviews, 1999, 39(1): 1−23.

[2] DAHOTRE N B, MCCAY T D, MCCAY M H. Laser processing of a SiC/Al-alloy metal matrix composite [J]. Journal of Applied Physics, 1989, 65(12): 5072−5077.

[3] DAHOTRE N B, GOPINATHAN S, MCCAY M H, MCCAY T D, SHARP C M. An evaluation of strength of pulsed laser welded SiC particulates reinforced Al-alloy metal matrix composite [C]//Light-weight Alloys for Aerospac Applications II. New Orleans: The Minerals, Metals and Materials Society, 1991: 313−326.

[4] ELLIS M B D. Joining of aluminum based metal matrix composites [J]. International Materials Reviews, 1996, 41(2): 41−58.

[5] WANG H M, CHEN Y L, YU L G. 'In-situ' weld-alloying/laser beam welding of SiC_p/6061Al MMC [J]. Materials Science and Engineering A, 2000, 293(1−2): 1−6.

[6] CHEN Y B, ZHANG D K, NIU J T, JI G J. In-situ reinforcing effect of Ti on aluminum matrix composite during laser beam welding [J]. Applied Laser, 2002, 22(3): 320−322. (in Chinese)

[7] VIJAY S J, MURUGAN N. Influence of tool pin profile on the metallurgical and mechanical properties of friction stir welded Al-10wt.% TiB_2 metal matrix composite [J]. Materials and Design, 2010, 31(7): 3585−3589.

[8] NAHED E M, TAHA M A, JARFORS A E W, FREDRIKSSON H. On the reaction between aluminum, K_2TiF_6 and KBF_4 [J]. Journal of Alloys and Compounds, 1999, 292(1−2): 221−229.

[9] KOH Y H, LEE S Y, KIM H. Oxidation behavior of titanium boride at elevated temperatures [J]. Journal of America Ceramic Society, 2001, 84(1): 239−241.

[10] CUI H C, LU F G, TANG X H, YAO S. Research on laser full-penetration welding in situ TiB_2 particulate reinforced ZL101 composites [J]. Advanced Materials Research, 2010, 97−101: 3967−3973.

[11] ZHU H G, WANG H Z, GE L Q, CHEN S, WU S Q. Formation of composites fabricated by exothermic dispersion reaction in Al-TiO_2-B_2O_3 system [J]. Transactions of Nonferrous Metals Society of China, 2007, 17(3): 590−594.

[12] BINNEWIES M, MIKE E. Thermochemical data of elements and compounds, second, revised and extended edition [M]. Weinheim: Wiley-VCH Verlag GmbH, 2002: 861−863.

[13] ARMSTRONG D R. The electronic structure of the first-row transition-metal diborides [J]. Theoretica Chimica Acta, 1983, 64(2): 137−152.

[14] SKOROKHOD V V, KRSTIC V D. Processing, microstructure, and mechanical properties of B_4C-TiB_2 particulate sintered composites. Part II: Fracture and mechanical properties [J]. Powder Metallurgy and Metal Ceramics, 2000, 39(9−10): 504−513.

激光焊接颗粒增强铝基复合材料中 TiB_2 颗粒的演变行为

孟 超，崔海超，芦凤桂，唐新华

上海交通大学 材料科学与工程学院，上海市激光制造与材料改性重点实验室，上海 200240

摘 要：研究大功率激光器焊接 TiB_2 颗粒增强铝基复合材料时 TiB_2 粒子的演变行为。采用 X 射线衍射(XRD)、扫描电镜(SEM)及能谱(EDS)分析焊缝内粒子的物相、热力学过程及形貌特征；同时对 TiB_2 和铝基体的界面反应进行讨论。结果表明：当 TiB_2 团簇尺寸大于激光光斑直径时，焊缝中部的 TiB_2 粒子会熔融在一起，较大尺寸的 TiB_2 会发生断裂；当与铝熔体接触后，熔化后的 TiB_2 粒子会与 Al 发生反应生成 Al_3Ti 和 AlB_{12}，并且焊缝中部的界面反应比焊缝边缘的剧烈。

关键词：金属基复合材料；TiB_2 粒子；激光焊接；界面反应

(Edited by Wei-ping CHEN)